HIPPOCAMPAL SURFACE ANALYSIS USING SPHERICAL HARMONIC FUNCTION APPLIED TO SURFACE CONFORMAL MAPPING

Boris Gutman[1], *Yalin Wang*[1,2], *Lok Ming Lui*[1], *Tony F. Chan*[1], *Paul M. Thompson*[2]

[1] Department of Mathematics, University of California, Los Angeles, CA USA
[2] Department of Neurology, UCLA Medical School, Los Angeles, CA USA
ylwang@math.ucla.edu

ABSTRACT

Using spherical harmonics of an inverse conformal map, we compared hippocampal surfaces of sixteen Alzheimer (AD) and fourteen control subjects. Hippocampal surfaces were conformally mapped to a sphere. Maps were regularly sampled and exact, high-degree spherical harmonic transforms of the inverse maps were computed. Using the transforms shape descriptors corresponding to the degree of the harmonics and invariant to translation, rotation, and scale were obtained and normalized against sample mean. Two-dimensional visualizations of the shape descriptors were indicative of global as well as local shape features of hippocampal surfaces. These descriptors are potentially useful for visual detection of global patterns and creation of population-based, probabilistic, disease-specific digital atlases, especially for comparison of global shape features.

1. INTRODUCTION

Recent studies have confirmed a long-observed correlation between changes in hippocampal shape and volume, and Alzheimer disease. Csernansky et al. [1] have found shape analysis methods that could potentially predict the onset of symptoms using high dimensional diffeomorphic transformations of a neuroanatomical template. Goldman et al. [2] have found that some patients with confirmed Alzheimer sometimes show few or no symptoms throughout much of their lives. Thus, changes in hippocampal shape characteristic of Alzheimer may take place years before patients show symptoms. Others [3] have even suggested the possibility of drug treatments capable of preventing or significantly slowing the progression of the disease. All these studies suggest a future need for accurate methods of analyzing local as well as global features of hippocampal shape. In our study, we compared the shapes of 14 left and 14 right hippocampi of control subjects with 16 left and 16 right hippocampi of Alzheimer subjects using spherical harmonic transform applied to surface conformal mapping. The procedure went as follows: (1) Triangulation meshes were reconstructed from 3-D T1 weighted SPGR (spoiled gradient) MRI images, by using an active surface algorithm that deforms a mesh onto the hippocampal surface [4]. (2) The meshes were then conformally mapped to a 2-sphere according to [5] and regularly sampled using linear interpolation, thus creating a spherical parameterization of the mesh. (3) A fast spherical harmonic transform algorithm (FST) was then performed on the regularly sampled meshes according to [6]. (4)Lastly, rotationally invariant shape descriptors were calculated, normalized for easy visual analysis and plotted in $\mathbb{R}^2$. We hope these two-dimensional visualizations of global shape descriptors will serve as a guide for future statistical analysis similar to that in [1] and the creation of disease-specific brain atlases as in [7].

2. PREVIOUS WORK

Various methods have been employed in the field of brain submanifold shape analysis. Gerig et al. [8] used spherical harmonics to compute mean squared distance between lateral ventricles of twins as a measure of pairwise shape difference by normalizing coefficients with respect to volume and applying Parseval's equation. Although mathematically elegant, this method involves much computational error due to irregularity of sample points. This is because spherical harmonic coefficients are approximated using a least squares solution. Another method is a high dimensional diffeomorphic map directly from a subject manifold onto an exemplar target manifold following Miller [9]. With this method, manifolds are divided into subregions and an overall mean transformation between all subjects and the target manifold is found for each of (usually) many thousands of points. Then, using the mean transformation, the mean manifold is constructed. Thus, the perpendicular displacement between each subject's surface and the overall mean for each subregion is calculated as a measure of shape variation. Csernanksi et al. [1] have employed this method in their study of Alzheimer's.

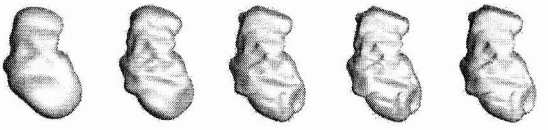

Fig. 1. Low-Pass Filtering: (a) through (d) are hippocampal surfaces reconstructed from harmonics up to degree 10, 20, 63 and 127, respectively. (e) is the original hippocampus

Use of spherical harmonic shape descriptors as initial representation of shape is advantageous to methods involving neuroanatomical templates in that the transform is independent of any population-based averages and that it describes global shape features in addition to locally detailed features. Figure 1 illustrates this property: lower-order spherical harmonics correspond to the major shape features of a hippocampus, while those of higher order correspond to noise and local features. Further, the analogue of a template in this method is a fixed target space, the sphere, which eliminates error due to variability of subject-based templates. As shown in [5], the conformal map onto the sphere is invariant to the specifics of triangulation and rotation. That spherical harmonics-based shape descriptors are also rotationally invariant in effect guarantees rotational invariance throughout the entire procedure of our method. In addition, the regularity of sampled grid points allows for a fast calculation of spherical harmonic coefficients which are exact up to numerical error associated

The 18th International Conference on Pattern Recognition (ICPR'06)
0-7695-2521-0/06 $20.00

with floating-point implementation.

3. CONFORMAL MAPPING ONTO THE 2-SPHERE

In this section we give the idea behind the conformal mapping algorithm following X. Gu, Y. Wang, et al. [5]. The idea is to first find a homeomorphism $\overrightarrow{f} : M \rightarrow \mathbb{S}^2$ (monomorphism between two topological spaces that is continuous in both directions) and then optimize it by minimizing harmonic energy. Here M is the manifold represented by a triangulation mesh of the object surface embedded in $\mathbb{R}^3$, defined by , (K, g) where K is a simplicial complex and $g : |K| \rightarrow \mathbb{R}^3$ is a function mapping the vertices of K to $\mathbb{R}^3$. For simplicity, consider a scalar piecewise-linear continuous function $f : M \rightarrow \mathbb{R}$. Let $u, v \in K$ be vertices, $\{u, v\} \in K$ the edge formed by u, v. (Here, we approximate all functions on M by continuous piecewise linear (PL) functions. Thus, the range-space of the conformal map is also a triangulation mesh.) Define the inner product on the space of PL functions by $< f, g >= \frac{1}{2} \sum_{\{u,v\} \in K} k_{u,v}(f(u) - f(v))(g(u) - g(v))$, where $k_{u,v}$ is string energy. By choosing the correct string energy constants, harmonic energy is defined by $E(f) =< f, f >= \sum_{\{u,v\} \in K} k_{u,v}||f(u) - f(v)||^2$. Vector functions on M to are defined by $\overrightarrow{f} = (f_1, f_2, f_3)$. Vector harmonic energy is $E(\overrightarrow{f}) = \sum_{i=1}^{3} E(f_i)$. Minimizing the harmonic energy ensures that the map is harmonic i.e. that the laplacian is equal to zero. That the map is harmonic guarantees its conformality. Here, the initial homeomorphism used is the Gauss map defined by $\overrightarrow{f}(v) = \overrightarrow{n}(v), v \in M$. For details on the algorithm minimizing harmonic energy and additional constraints placed on the function to ensure convergence as well as an explanation in a more general setting, see [5].

4. SPHERICAL HARMONICS

A function $f : \mathbb{S}^2 \rightarrow \mathbb{C}$ is a spherical harmonic if it is the eigenfunction of the Laplacian operator $\Delta f = \lambda f$ where λ is a scalar multiplier. A countable set of spherical harmonics provides an orthonormal basis for the space of square-integrable functions on the sphere $L^2(\mathbb{S}^2)$. If we parameterize the sphere with a latitudinal coordinate c and a colatitudinal coordinate p, spherical harmonics are expressed explicitly:

$$Y_l^m(\theta, \phi) = \sqrt{\frac{(2l+1)(l-m)!}{4(l+m)!}} P_l^m(cos\theta) e^{im\phi}$$

for the degree l and order m, where l and m are integers with $|m| < l$. Here, $P_l^m(cos\theta)$ is the associated Legendre polynomial $P_l^m(cos\theta) = \frac{(-1)^m}{2^l l!}(1-x^2)^{\frac{m}{2}} \frac{d^{m+1}}{dx^{m+1}}(x^2-1)^l$, which is a solution to the associated Legendre differential equation. Let f be in $L^2(\mathbb{S}^2)$. For a given order l and degree m, a spherical harmonic coefficient is defined by $\widehat{f}(l, m) =< f, Y_l^m >$, where $< f, g >$ is the usual L^2 inner product in spherical coordinates. The spherical harmonic expansion is the series $f(\theta, \phi) = \sum_{l=0}^{\infty} \sum_{m=-l}^{l} \widehat{f}(l, m) Y_l^m(\theta, \phi)$. The set of all coefficients $\widehat{f}(l, m)$ is called the spherical harmonic transform of f. In practice, the transform is computed with a fast algorithm described in [6], which relies on regular mesh sampling. The transform is only computed up to a certain degree $l < B$, where the limit B is called the bandwidth.

A consequence of Parseval's equation is that any function in $L^2(\mathbb{S}^2)$ is uniquely determined by its spherical harmonic coefficients, implying that linear transformations (scaling, rotation, translation) in the object space alter an object's spectrum. Thus, further registration is needed to make each individual coefficient completely invariant to linear transformations. While translational invariance is achieved easily, rotational invariance will be the subject of the concluding section. For now, we have achieved a limited rotational invariance by simplifying the spectrum as described below.

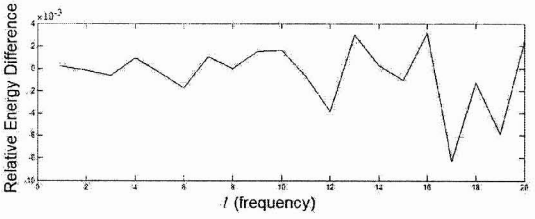

Fig. 2. Rotational invariance: A hippocampal surface was rotated 45 degrees around each axis, mapped conformally and decomposed into new spherical harmonics. The plot shows the relative difference between the new and the original descriptors: $[s(l) - s(l')]/s(l)$ versus degree l. Error is within 1%.

5. SPHERICAL HARMONIC ANALYSIS AND THE SURFACE CONFORMAL MAP

Let $\overrightarrow{f} : M \subset \mathbb{R}^3 \rightarrow \mathbb{S}^2$ be a conformal homeomorphism defined discretely by $\overrightarrow{f} = (f_1, f_2, f_3)$, as described in section (3), where M is a mesh representing the object. Let $\overrightarrow{f}^{-1} : \mathbb{S}^2 \rightarrow \mathbb{R}^3$ be the inverse map from the sphere onto the hippocampal surface, defined by the isomorphic property of the homeomorphism. We regularly sample $\overrightarrow{f}^{-1} = (f_1^{-1}, f_2^{-1}, f_3^{-1})$ using a matching area algorithm and linear interpolation, and apply the FST to each scalar component of the inverse map. This amounts to projecting the inverse of the discrete conformal map onto a finite-dimensional subspace of $L^2(\mathbb{S}^2)$. The result is a set of vector spherical harmonic coefficients in $\mathbb{C}^3$

$$\widehat{\{\overrightarrow{f}^{-1}(l, m)} = \{\widehat{f_1^{-1}}(l, m), \widehat{f_2^{-1}}(l, m), \widehat{f_3^{-1}}(l, m) || m| \leq l \leq B\}\}$$

, where B is the bandwidth. The spectrum simplification necessary for rotational invariance comes from two key observations. One is that the norm of a function in $L^2(\mathbb{S}^2)$ does not change with rotation. The other is that for a spherical function $p_l \in Span\{Y_l^{-l}, Y_l^{-l+1}, ..., Y_l^l\}$, given an element of the rotation group $g \in SO(3)$ and its associated operator $\Lambda(g)$, the transformed function remains in the same subspace of $L^2(\mathbb{S}^2)$: $\Lambda(g)(p_l) \in Span\{Y_l^{-l}, Y_l^{-l+1}, ..., Y_l^l\}$. Thus,

$$\sum_{m=-l}^{l} |\widehat{p_l}(l, m)|^2 = ||p_l||_2^2 = ||\Lambda(g)(p_l)||_2^2 = \sum_{m=-l}^{l} |\Lambda(g)(p_l)(l, m)|^2$$

Further, the linearity of $\Lambda(g)$ implies $f(\theta, \phi) = \sum_{l=0}^{B-1} p_l \Rightarrow \Lambda(g)[f(\theta, \phi)] = \sum_{l=0}^{B-1} \Lambda(g)(p_l)$. This motivates the following definition. Returning to our original notation, we define spherical harmonic shape descriptors $s(l) = \sum_{i=1}^{3} \sum_{m=-l}^{l} ||\widehat{f_i}^{-1}(l, m)||^2$ to be the squared Euclidean norms of squared L^2-norms of the vector

0-7695-2521-0/06 $20.00

inverse maps. In view of the three observations above, these descriptors should be invariant to rotation, as each of the inner sums is theoretically invariant. It is also possible to make the coefficients translationally invariant by simply disregarding the degree-zero coefficient, which is alone responsible for translation. Thus, we produce a quasi-unique multi-resolution global shape representation. Now, surface comparison is possible directly in the simplified spectrum domain without registration.

6. EXPERIMENTAL RESULTS

Our experimental results confirm rotational invariance (see fig. 2) up to discretization and sampling error. Relative error due to a random rotation is within 1 %. Although the initial descriptors are not based on any population averages, here we use sample-based normalization constants $C(l) = \frac{1}{N}\sum_{i=1}^{N}\sum_{k=1}^{B-1} s_i(k)/s_i(l)$, where N is the total number of meshes, $s_i(k)$ is the kth degree descriptor of the ith mesh and B is the bandwidth of the transform (note that the degree-zero coefficient is omitted). Normalized shape descriptors $n(l) = s(l)C(l)$ provide a measure of the ratio of the size of major features to smaller protrusions and highly localized features of an object against the sample mean. For example, the first degree harmonics form the "main ellipsoid" of the object (see [10]). Suppose $n(1)$ of a particular hippocampus is smaller in comparison with its lower degree $n(l)$ for $l \neq 1$. We conclude that as compared to the sample mean, this hippocampus has more major curves and large protrusions with respect to its "main body." Shape descriptors are normalized further with respect to a fixed lower-degree descriptor for scale invariance. Thus, the main novelty of our method is that it provides an invariant multiresolution representation while making comparisons across populations and frequencies meaningful. Figure 3 illustrates 2-D visualizations of normalized shape descriptors similar to the example above. Figure 4 shows the original hippocampi described by the visualizations in Figure 3.

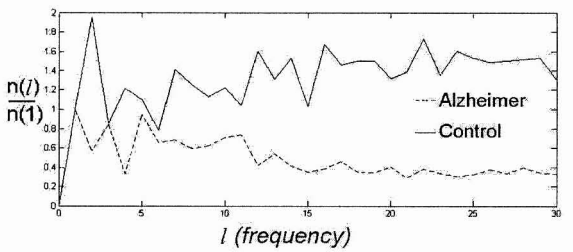

Fig. 3. Plots of normalized descriptors for two hippocampi: higher relative magnitude in lower frequency descriptors of the solid line indicates a greater presence of low-frequency curves in the control hippocampus.

We ran a 3-way ANOVA on normalized descriptors with hemisphere, diagnosis and frequency as factors. Only descriptors up to frequency 15 were considered, as they generate over 98 % of hippocampal harmonic energy. Further, because only a subset of the normalized spectrum was used, the sample-based constants are objective. Most notably, the test yielded significant results for diagnosis (df=1, F=4.061, α=.044), and interaction between diagnosis and hemisphere (df=1, F=7.520, α=.006). Other significant factors include hemisphere (df=1, F=6.429, α=.011), and interaction between frequency and hemisphere (df=14, F=2.694, α=.001). Here, "df" stands for "degrees of freedom," "F" is the value from the F-distribution (a continuous distribution which arises when comparing variances between two samples) based on sums of squares and "α" is the tail of the distributin at the given F-value. When examining the ANOVA, we found that frequencies 2, 6, 8, 12, 14 and 15 give the most significant interaction between diagnosis and hemisphere. We computed the average of frequency-wise differences in descriptor magnitude between the right and left hemispheres for each subject only for the frequencies above. An independent samples t-test of the differences average between cntrol and AD subjects confirms their significance: (df=28,t=-2.692, P=.012). In particular, we noted that while the average was slightly higher among AD subjects in the right hemisphere, it was significantly lower in the left comapred to control subjects. This is consistent with [1], where significant reduction in surface area was found specifically in the lateral zone of the left hippocampus.

7. CONCLUSION AND FUTURE WORK

Our spherical harmonic shape descriptors were found to be a good means of quantifying shape features in hippocampal surfaces. These rotationally and translationally invariant descriptors have potential to be quite useful in creating population-based disease-specific brain atlases. Further, an advantage of using spectrum-based descriptors lies in their ability to quantify aspects of global shape undetectable with region-by-region comparison to population averages. In experiments, our global metric was found to have comparable sensitivity to local deformations as some localized metrics described above, giving purpose to future refinements of our method.

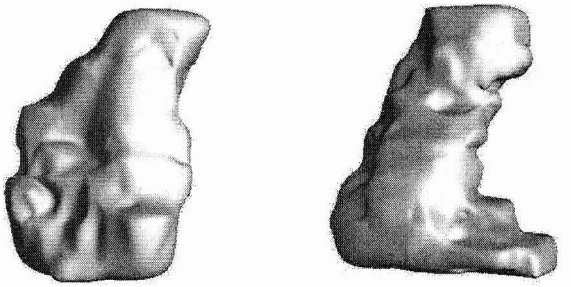

Fig. 4. Two original hippocampal surfaces: (a) is a left hippocampus of a female Alzheimer subject and (b) is a left hippocampus of a female control subject, corresponding to Figure 3.

To further develop use of spherical harmonics as a means of shape representation in the future, we would like to:

(1)Develop a direct registration method via spherical cross-correlation

(2)Develop a spherical harmonic representation which is intrinsically optimal with respect to the conformal structure of the surface, thus integrating the theory of spherical harmonics with global conformal mapping

(3)Develop a better understanding of the interplay between spherical harmonic shape representation and moments expressed in terms of shape characteristics, as can be analogously done for the 2-D case [10].

(4)Test more hippocampal surfaces with our method. The Laboratory on Neuro Imaging at UCLA has kindly provided us with more

than 122 new hippocampal models. To make the first step in this direction, we are currently transforming the models into mesh format.

8. REFERENCES

[1] J. G. Csernansky, L. Wang, J. Swank, J. P. Miller, M. Gado, D. McKeel, M. I. Miller, and J. C. Morris, "Preclinical detection of Alzheimer's disease: hippocampal shape and volume predict dementia onset in the elderly," Neuroimage. Vol 25 Issue 3, pp 783-792, 15 April 2005

[2] W. P. Goldman, J. L. Price, M. Storandt, E. A. Grant, D. W. McKeel Jr., E. H. Rubin and J. C. Morris, "Absence of cognitive impairment or decline in preclinical Alzheimer's disease," Neurology 56, pp. 361-367, 2001.

[3] N. Bodick, F. Forette, D. Hadler, R. J. Harvey, P. Leber, I. G. McKeith, P. J. Riekkinen, M. N. Rossor, P. Scheltens, S. Shimohama, R. Spiegel, S. Tanaka, L. J. Thal, Y. Urata, P. Whitehouse and G. Wilcock, "Protocols to demonstrate slowing of Alzheimer disease progression." The Disease Progression Sub-Group, Alzheimer Dis. Assoc. Disord. (Suppl 3), pp. 50-53. November 1997

[4] P. M. Thompson and A. Toga, "A framework for computational anatomy," in Comput. Visual. Sci., vol. 5, 2002, pp. 1-12

[5] X. Gu, Y. Wang, T. F. Chan, P. M. Thompson, and S. Yau "Genus Zero Surface Conformal Mapping and Its Application to Brain Surface Mapping" IEEE Transactions on Medical Imaging, Vol. 23, No. 8, p. 949, August 2004

[6] D. Healy, D. Rockmore, P. Kostelec, and S. Moore, "Ffts for the 2-sphere-Improvements and variations," J. Fourier Anal. Applicat., vol. 9, no. 4, pp. 341-385, 2003.

[7] P. Thompson, M. Mega, C. Vidal, J. Rapoport, and A. Toga, "Detecting disease-specific patterns of brain structure using cortical pattern matching and a population-based probabilistic brain atlas," in Proc.17th Int. Conf. Information Processing in Medical Imaging (IPMI2001), Davis, CA, June 18-22, 2001, pp. 488-501.

[8] G. Gerig, M. Styner, D. Jones, D. Weinberger, and J. Lieberman, "Shape analysis of brain ventricles using spharm," presented at the IEEE Workshop on Mathematical Methods in Biomedical Image Analysis (MMBIA'01), Kauai, HI, December 2001.

[9] M. I. Miller, "Computational anatomy: shape, growth, and atrophy comparison via diffeomorphisms" Neuroimage Vol. 23, Supp 1, pp. S19-S33, 2004.

[10] C. Brechbuhler, G. Gerig, and O. Kubler, "Surface parametrization and shape description," Proc. SPIE (Visualization Biomed. Comp. 1992), vol. 1808, pp. 80-89, 1992.

[11] A. Cuyt, J. Sijbers, B. Verdonk, D. Van Dyck, "Region and Contour Identification of Physical Objects" Appl. Num. Anal. Comp. Math. 1, No. 2, 343 - 352, 2004

[12] J. G. Csernansky, S. Joshi, L. Wang, J. W. Haller, M. Gado, J. P. Miller, U. Grenander, and M. I. Miller "Hippocampal morphometry in schizophrenia by high dimensional brain mapping," Proc. Natl. Acad. Sci. USA Vol. 95, pp. 11406-11411, September 1998.

[13] P. M. Thompson, M.S. Mega, R.P. Woods, C.I. Zoumalan, C.J. Lindshield, R.E. Blanton, J. Moussai, C.J. Holmes, J.L. Cummings, A.W. Toga "Cortical change in Alzheimer's disease detected with a disease-specific population-based brain atlas." Cereb Cortex. January 2001; 11(1):1-16.

[14] M. Kazhdan, T. Funkhouser, S. Rusinkiewicz "Rotation Invariant Spherical Harmonic Representation of 3D Shape Descriptors" Proc. of Symposium on Geometry Processing pp. 167-175, June 2003

0-7695-2521-0/06 $20.00 © 2006